ISSN 0389-4010
UDC 533. 6. 011. 3
533. 6. 04

TECHNICAL REPORT OF NATIONAL AEROSPACE LABORATORY

TR-996T

Computational and Experimental Research on Buffet Phenomena of Transonic Airfoils

Naoki HIROSE and Hitoshi MIWA

September 1988

NATIONAL AEROSPACE LABORATORY

CHŌFU, TOKYO, JAPAN

Computational and Experimental Research on Buffet Phenomena of Transonic Airfoils*

Naoki HIROSE** and Hitoshi MIWA**

ABSTRACT

Buffet phenomena on supercritical airfoils were investigated both experimentally and numerically. The experiment was done for NACA0012 and KORN 75-06-12 airfoils using a high-speed Schlieren VTR and pressure transducers. The analysis shows significant effects of the geometries and the Reynolds number. A 2-D N-S code was used to predict these phenomena. The result shows the macro-scale effects of airfoil geometry, Reynolds number and transition. A fine structure of the motion such as the periodic trailing edge pressure history was captured. The basic frequency of the buffet motion agrees well with the experiment.

概　　要

超臨界翼型の遷音速バフェット現象の実験的および計算空気力学的解析を行った。実験は従来型の翼型 NACA0012と超臨界翼型 KORN75-06-12の２種類の翼型に対して航技研高レイノルズ数二次元風洞で行い，高速シュリーレン映像のヴィデオ録画と圧力変換器による圧力変動の測定を行った。その結果，翼型形状とレイノルズ数の著しい効果が明らかになった。また，２次元ナヴィエ・ストークス方程式に対する計算空気力学的方法による，このような現象の予知を試みた。数値解析の結果は，翼型形状，レイノルズ数，境界層遷移の空力特性等マクロなスケールへの影響を示し，さらに，後縁圧力の周期的な非定常特性などの微細構造を捕らえた。計算によるバフェットの基本周期は実験値と良い一致を示している。

本報告はこれらの研究の概要を抄訳取り纏め，国際理論応用力学連合 (IUTAM) 主催『シンポジウム・トランソニカムⅢ』（第３回遷音速空気力学シンポジウム，1988年５月24日～27日，西ドイツ，ゲッチンゲン市）で発表報告したものである。本研究の詳細報告は別途準備中の TR を参照されたい。

I. INTRODUCTION

Buffet phenomena in transonic flow are characterized by very complicated flow regime with shock wave oscillation, shock wave-induced boundary layer separation and separated vortex shedding behind the shock wave. This unsteady aerodynamic oscillation produces large unsteady aerodynamic forces which are not desirable. Therefore the prediction and the investigation of this phenomena in detail are quite important.

Experimental investigation is very difficult, because heavy unsteady load to the model and support during the wind blow is dangerous, and high quality measurements of unsteady pressure and flow field are required but they are hardly realized due to various adverse circumstances in

*Received 2, August, 1988
**The Aircraft Aerodynamics Division

facility and instrumentation. A few number of researches are reported in the past. McDevitt, Levy and Deiwert[1~3] made biconvex circular-arc airfoil experiment and compared its buffet behavior with Navier-Stokes computation. By the way, Deiwert's computation was the first Navier-Stokes analysis for practical subject at high Reynolds number and computed on ILLIAC-IV. Levy and Bailey[4] then computed buffet boundaries for NACA65-213 and Garabedian-Korn airfoils. Roos[5] made buffet experiment for Whitcomb and NACA0012 airfoils and investigated unsteady pressure field.

In Japan, since the construction of High-Reynolds Number 2-D Wind Tunnel (HR2DWT) in 1978, supercritical airfoils have been tested in this wind tunnel.[6] Also, a Navier-Stokes code was developed and code verification was made for NACA0012 and several supercritical airfoils.[7] For one practical purpose-airfoil, buffet boundary as well as static force data showed good agreement with each other.[8] Computation gave buffet frequency of 45 Hz while the energy power spectra measured in the wind tunnel showed a distinct peak at about 60 Hz nearly equal to the computed result.

In the present paper, a further investigation was made both experimentally and computationally to the buffet phenomena of NACA0012 and GARABEDIAN-KORN 75-06-12 airfoils. The latter abridged as KORN airfoil is a well-known supercritical airfoil and its design point is lift coefficient of 0.6 at Mach number of 0.75 with shockless pressure distribution. In the experiment, effects of Reynolds number on conventional and supercritical airfoils were examined. In computations, effects of Reynolds number, angle of attack, transition models on buffet mode were examined. Also comparison with experiment was made for KORN airfoil.

2. EXPERIMENTAL RESEARCH

2.1 Wind Tunnel and Procedures

Experiments were conducted in the NAL HR2DWT, a blow-down flow facility for airfoil testing. The test section is 30 cm wide and 100 cm high. A 25 cm-chord airfoil model is installed between the optical windows and supported by the rigid steel blocks outside the flow passage (Fig. 1.). The wind tunnel provides maximum Reynolds number 40 x 10^6 (at M = 0.8). Mach number range, 0.2 to 1.15, and running time, 9 to 100 sec.

Airfoil sections used were NACA0012 and KORN airfoils. Mach number range was 0.5 to

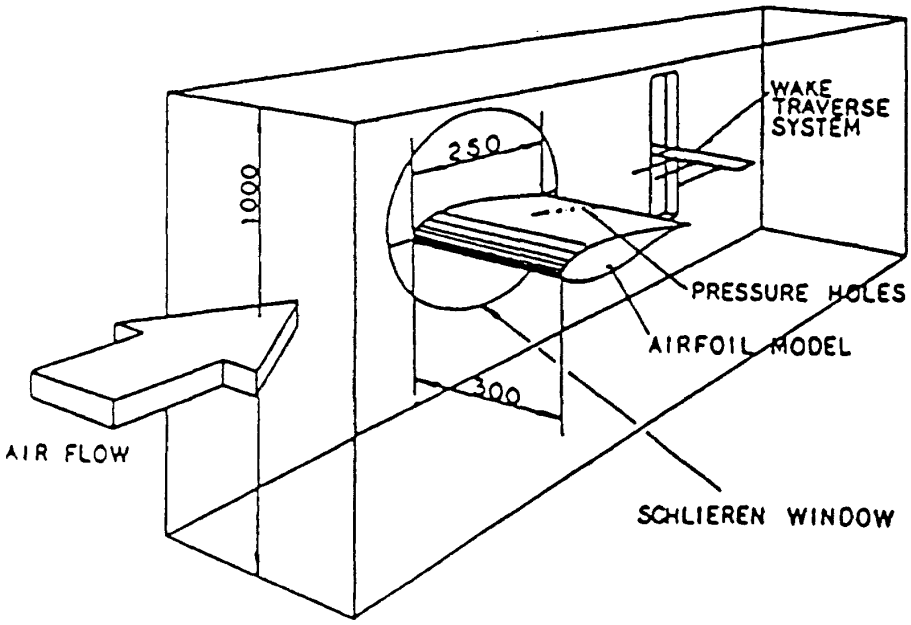

Fig. 1 HR2DWT schematics

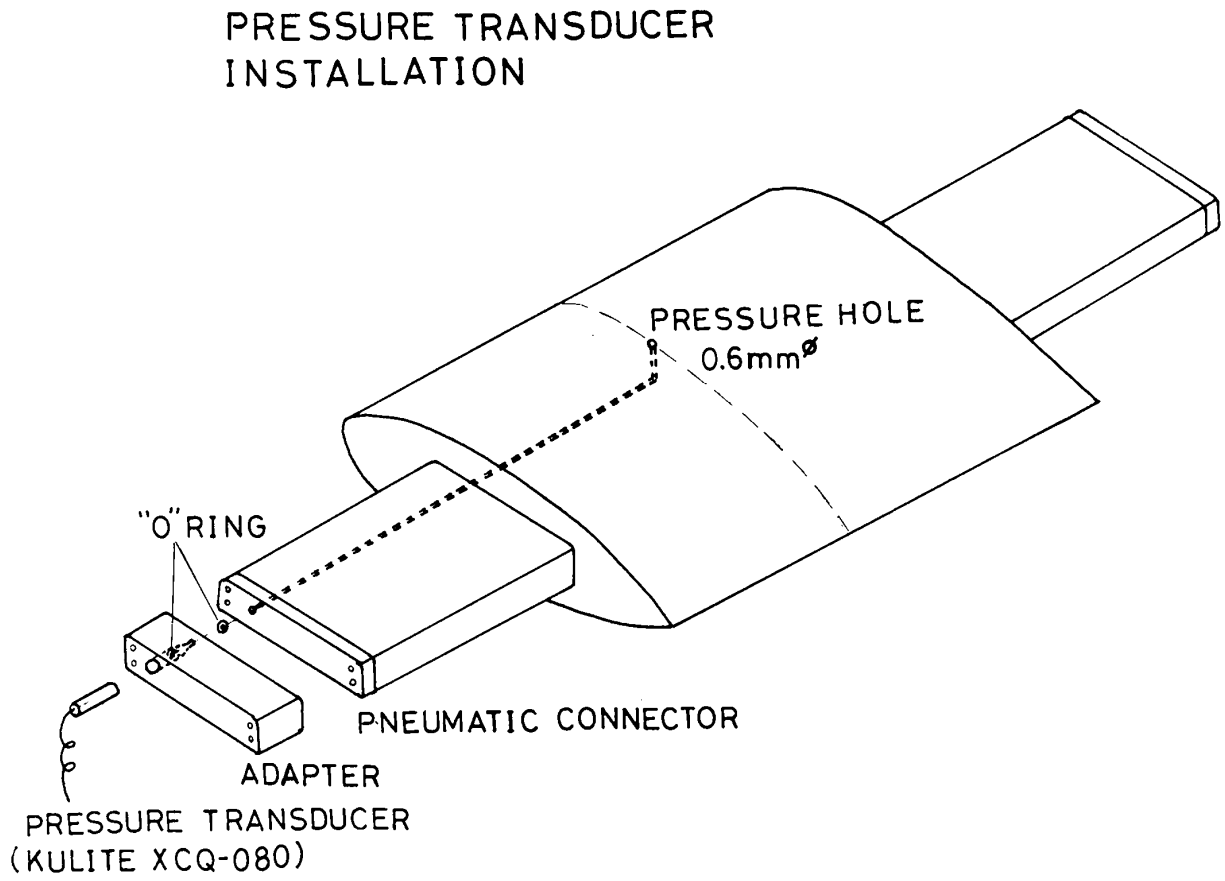

Fig. 2 Model and pressure transducer installation

0.85. Reynolds numbers were 6, 15 and 30 × 10^6. Pressure fluctuations at every 10% chord station were measured by small pressure transducers (KULITE XCQ-080) connected by adapter to the pneumatic connector located side of the model. Static pressure holes of diameter 0.6 mm were utilized for this purpose. Total of 10 points were measured (Fig. 2). The outputs of transducer signals were recorded by 14 channel analog data recorder. Pressure fluctuation at one wake point and one side-wall point above trailing edge and strain at model support section were also measured. Frequency response between the pressure hole and the transducer was checked beforehand. Maximum frequency of 200Hz can be measured within 90% of accuracy. R.M.S. level of the pressure fluctuation normalized to the dynamic pressure of the free stream, power spectra, and cross-correlations with trailing edge as the reference point were computed to see the time-space correlation of the separated vortices.

A high-speed camera and high-speed Video Tape Recorder (200 frames/sec) were also used to obtain optical measurement of shock wave movement and flow separaton patterns.

2.2 Results and Discussion

[SHOCK WAVE LOCATION]

Shock wave location obtained from VTR images is plotted against angle of attack with Mach number M as parameter for NACA0012 and KORN airfoils respectively in Figs. 3(a) and (b). Solid line is for Reynolds number, Re = 30 × 10^6 and dashed line for Re = 6 × 10^6. The shaded area shows unsteady shock wave oscillation, i.e. buffet area. At full buffet point, the amplitude of the shock wave movement increases with Reynolds number for both airfoils. The increment is greater for NACA0012 than KORN airfoil. Mach number dependency differs between two airfoils. In NACA0012 case, the amplitude of oscillation increases with Mach

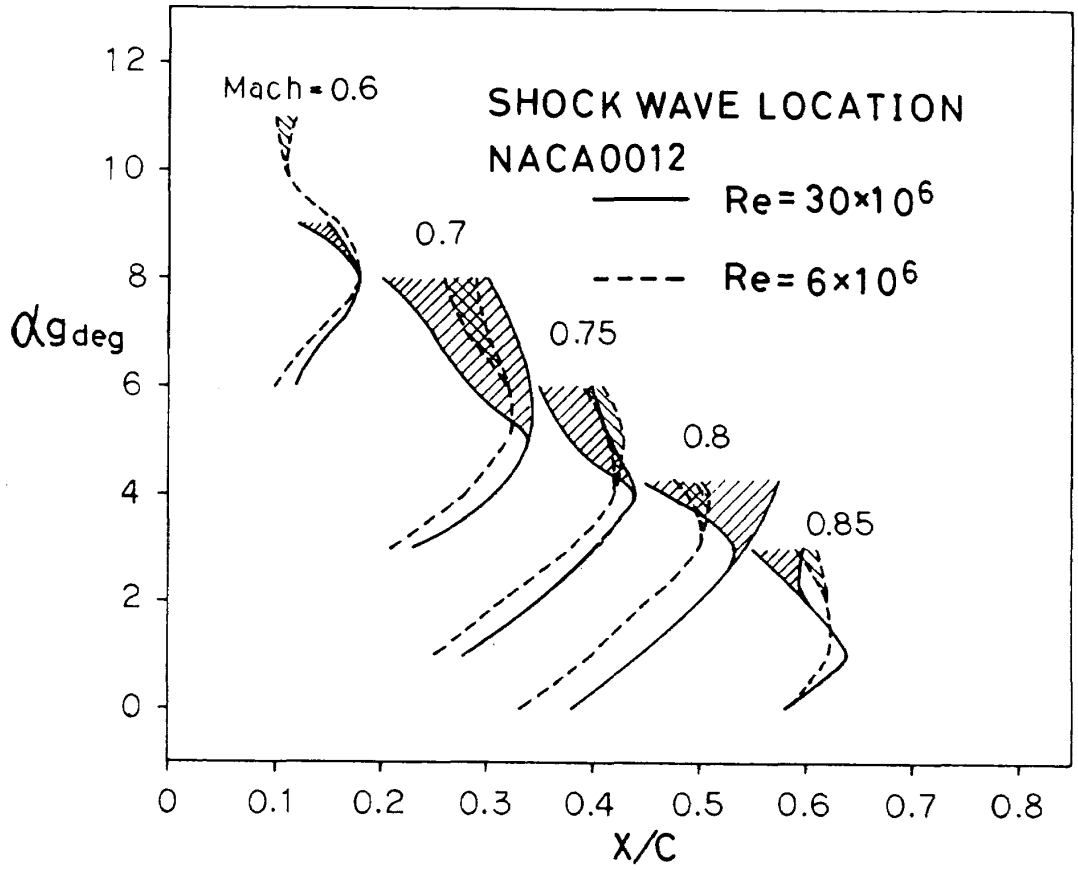

(a) NACA0012 airfoil

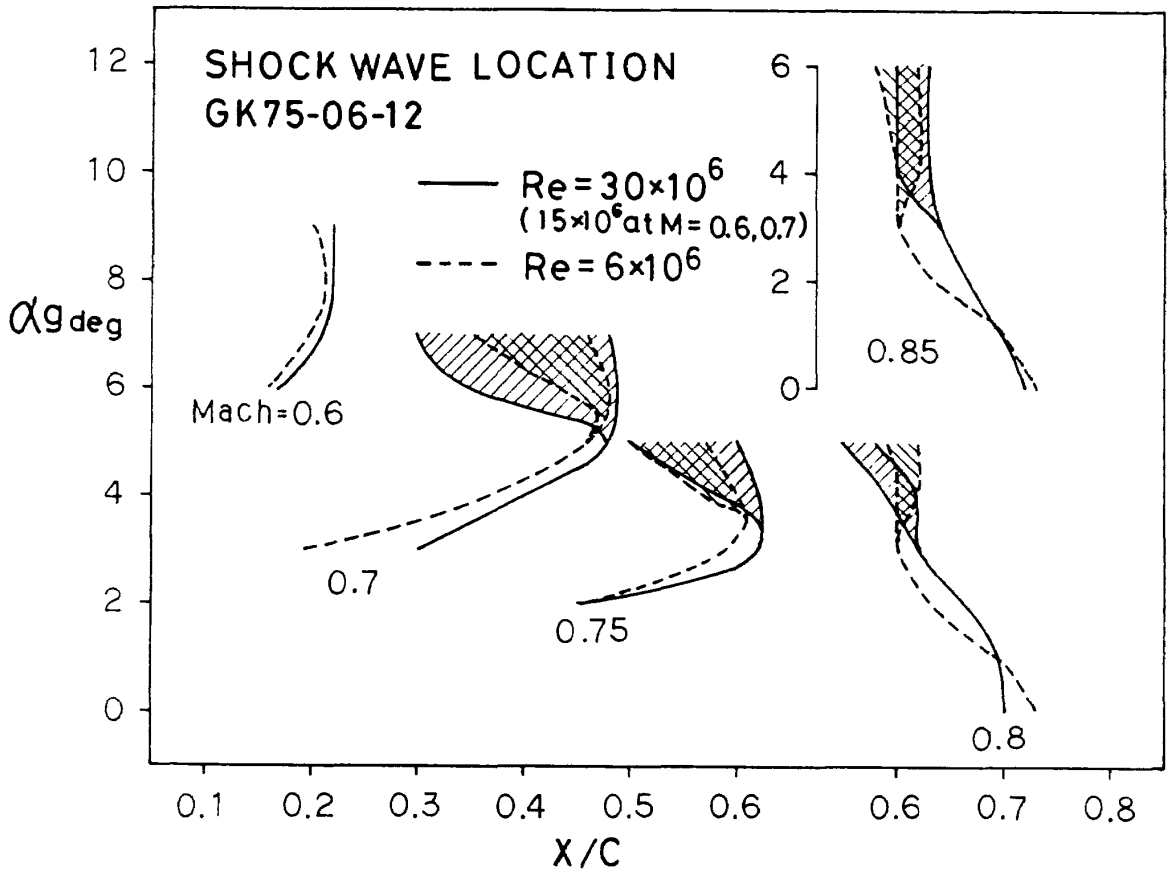

(b) KORN airfoil

Fig. 3 Shock wave locations

number while it decreases in KORN airfoil case. The largest oscillation occurs at M = 0.7 of supercritical airfoil case.

Shock wave is located rearward at high Reynolds number for both of airfoils when angle of attack is below buffet onset point but the situation reverses when buffet starts in NACA0012 case (Fig. 4 (a) and (b)).

[STRAIN AND TRAILING EDGE PRESSURE FLUCTUATION]

Strain at model support section and trailing edge fluctuation C_{PTE}' are closely related. The start of model vibration, i.e. buffet onset, corresponds with the start of C_{PTE}'. Significant buffet exists for all range of Mach number in NACA0012 case but it almost disappears when Mach number is increased to 0.85 in KORN case.

[FLUCTUATION PRESSURE ON AIRFOIL SURFACE]

Figure 5 shows pressure fluctuation distribution at Re = 30 × 10^6 with angle of attack as a parameter for both airfoils. Shock wave location is also shown. Pressure fluctuation peak point and shock location should coincide but it differs at angle of attack for buffet onset point. This was caused by that shock wave location was optically measured along line 10 mm above surface. Local minimum point of fluctuation can be observed just behind the shock wave which indicates the existence of separation bubble.

For low Reynolds number, pressure fluctuation is larger in KORN case than in NACA0012 case. As Reynolds number increases, pressure fluctuation decreases more in KORN case. This can be clarified by trailing edge pressure fluctuation C_{PTE}' shown in Fig. 6. Distinctive difference between the two airfoils are observed.

[POWER SPECTRA AND CROSS-CORRELATIONS]

Figure 7 shows power spectra and cross-correlations at M = 0.70, α = 6°, Re = 15 × 10^6 of NACA0012 airfoil. At low Reynolds number, peak of the power spectra lies at very low frequency (2.5 Hz). As Reynolds number increases, the peak position moves rearward and the peak frequency increases to 62.5 Hz. The spectra becomes broadband with various frequency

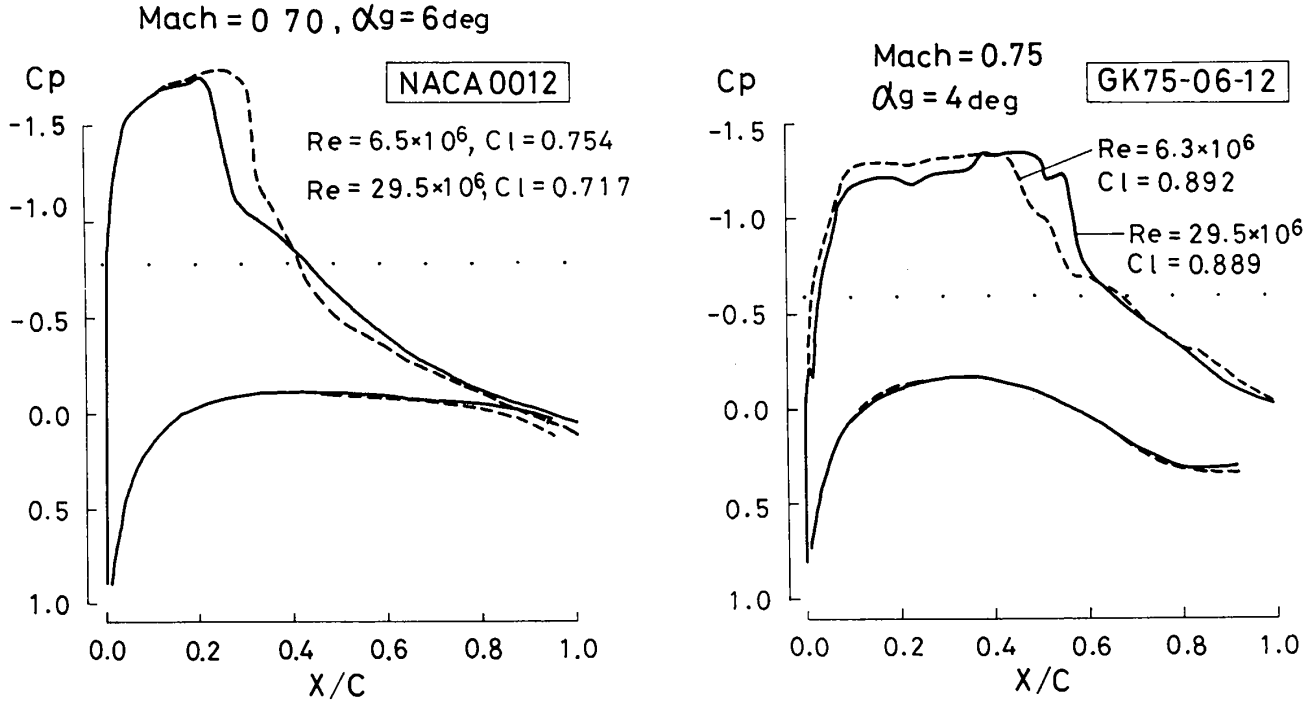

(a) NACA0012 airfoil, M = 0.70, α = 6°

(b) KORN airfoil, M = 0.75, α = 4°

Fig. 4 Surface pressure distributions at buffet range

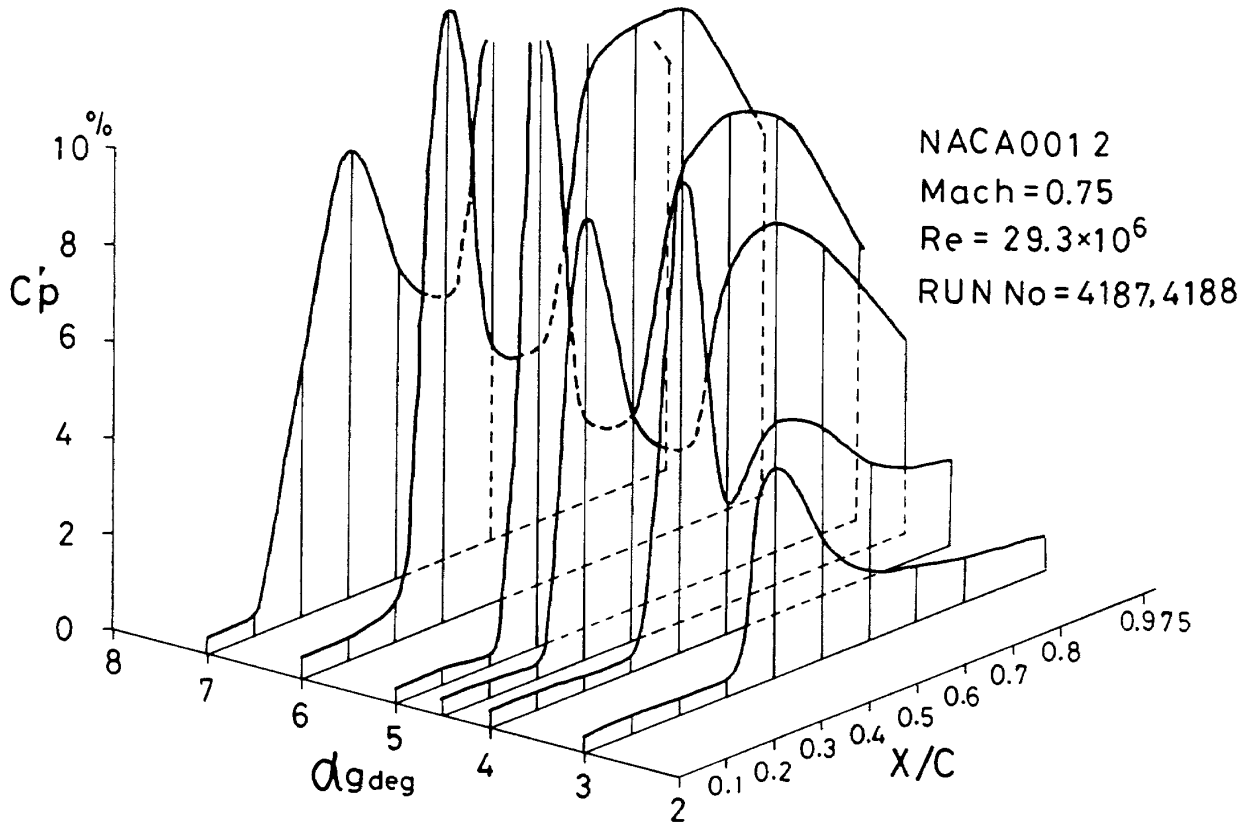

(a) NACA0012 airfoil

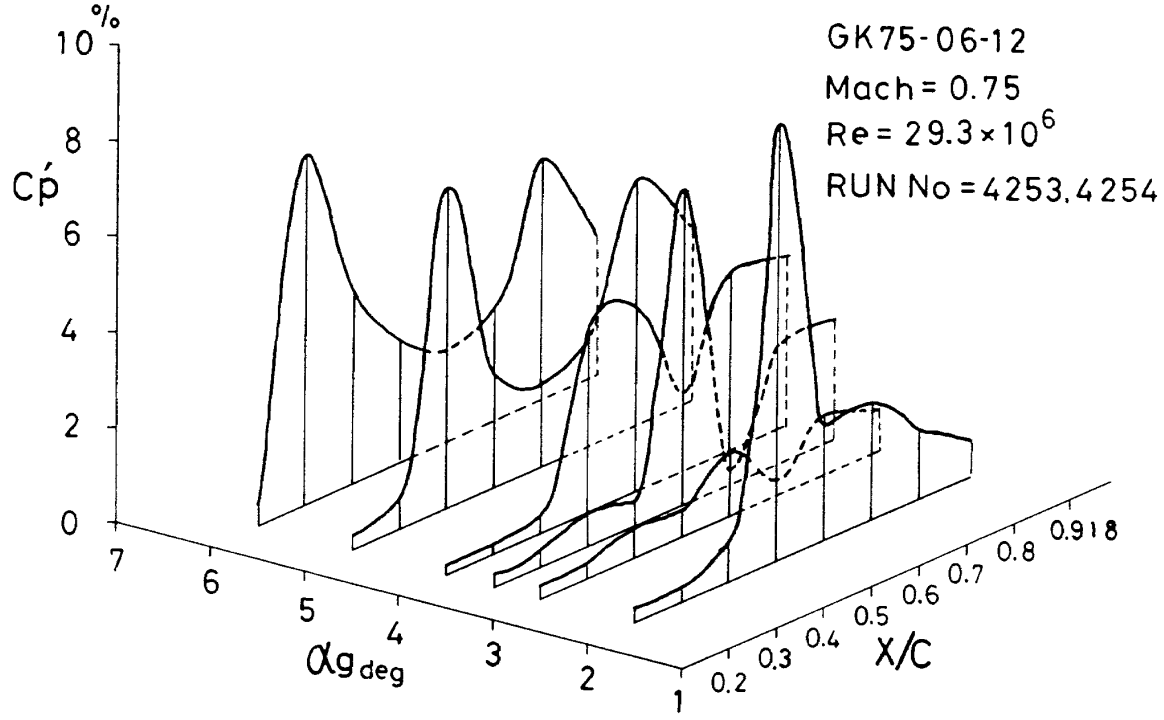

(b) KORN airfoil

Fig. 5 Pressure fluctuation distributions

components which means that various size of vortices exist. The Lag-time of the peak position of cross-correleation is negative. This indicates separated vortices from the foot of shoch wave moves streamwise. Correlation is high for high Reynolds number.

Power spectra and cross-correlations for KORN airfoil is shown in Fig. 8 at M = 0.75, $\alpha = 4^\circ$, Re = 30×10^6. At low Reynolds number, peak of the power spectra lies at very low frequency (5 Hz) as in NACA0012 case but with broad band both in frequency and space. As

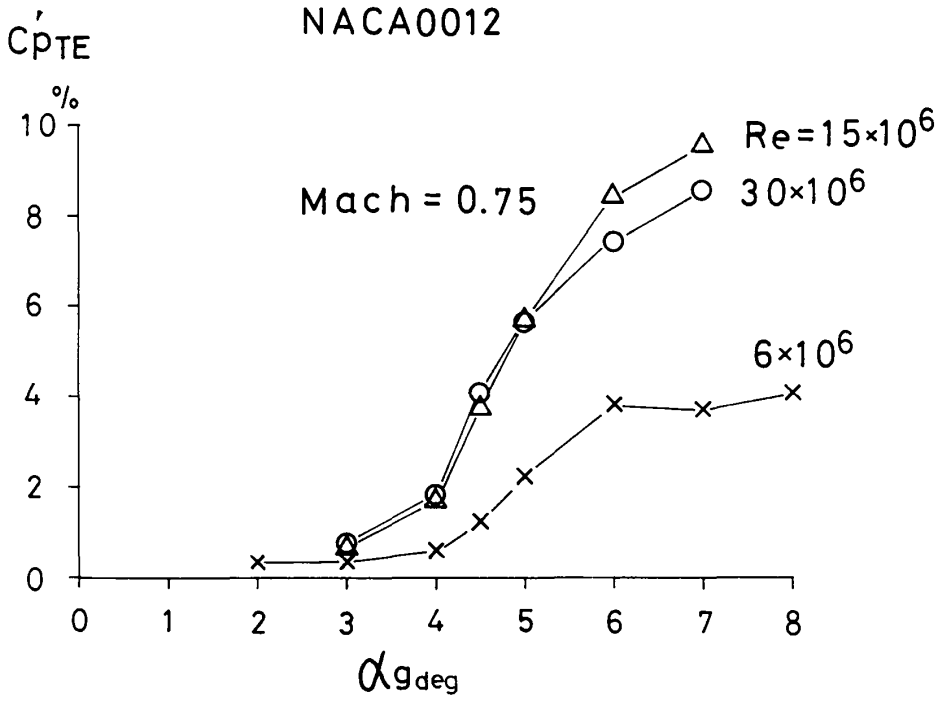

(a) NACA0012 airfoil, M = 0.75

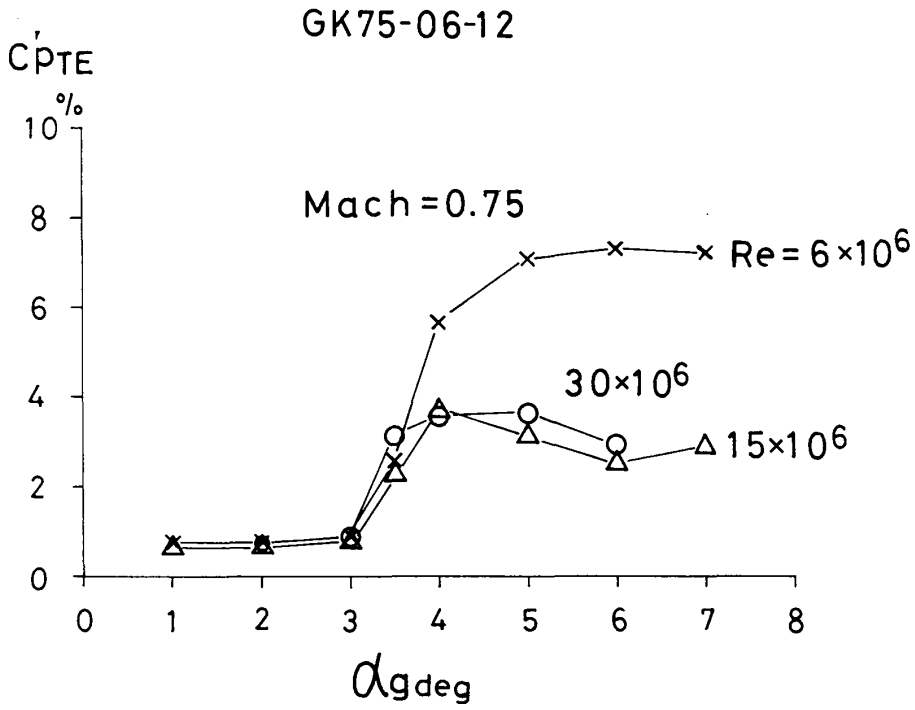

(b) KORN airfoil, M = 0.75

Fig. 6 Trailing edge pressure fluctuations

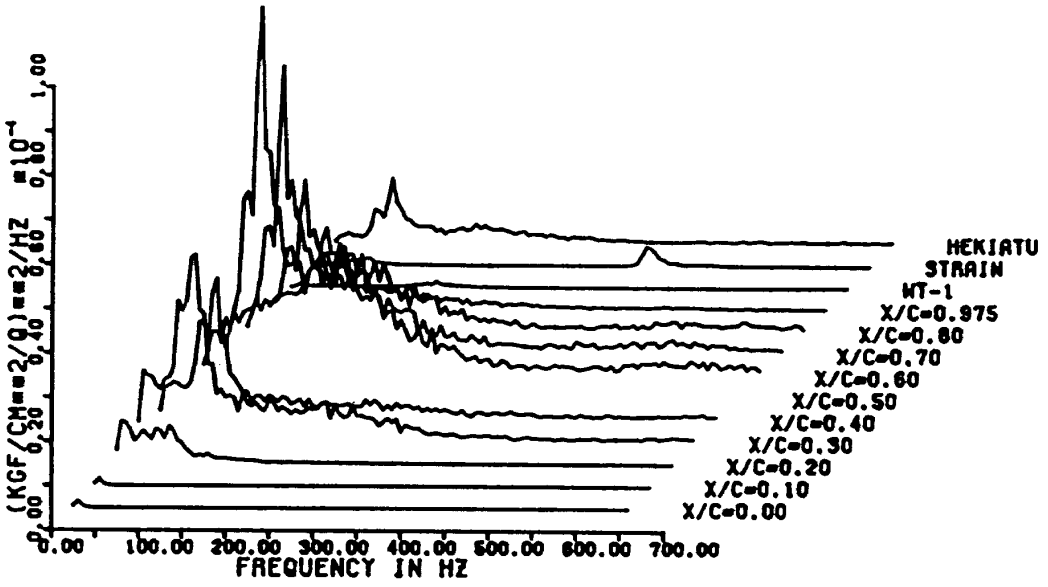

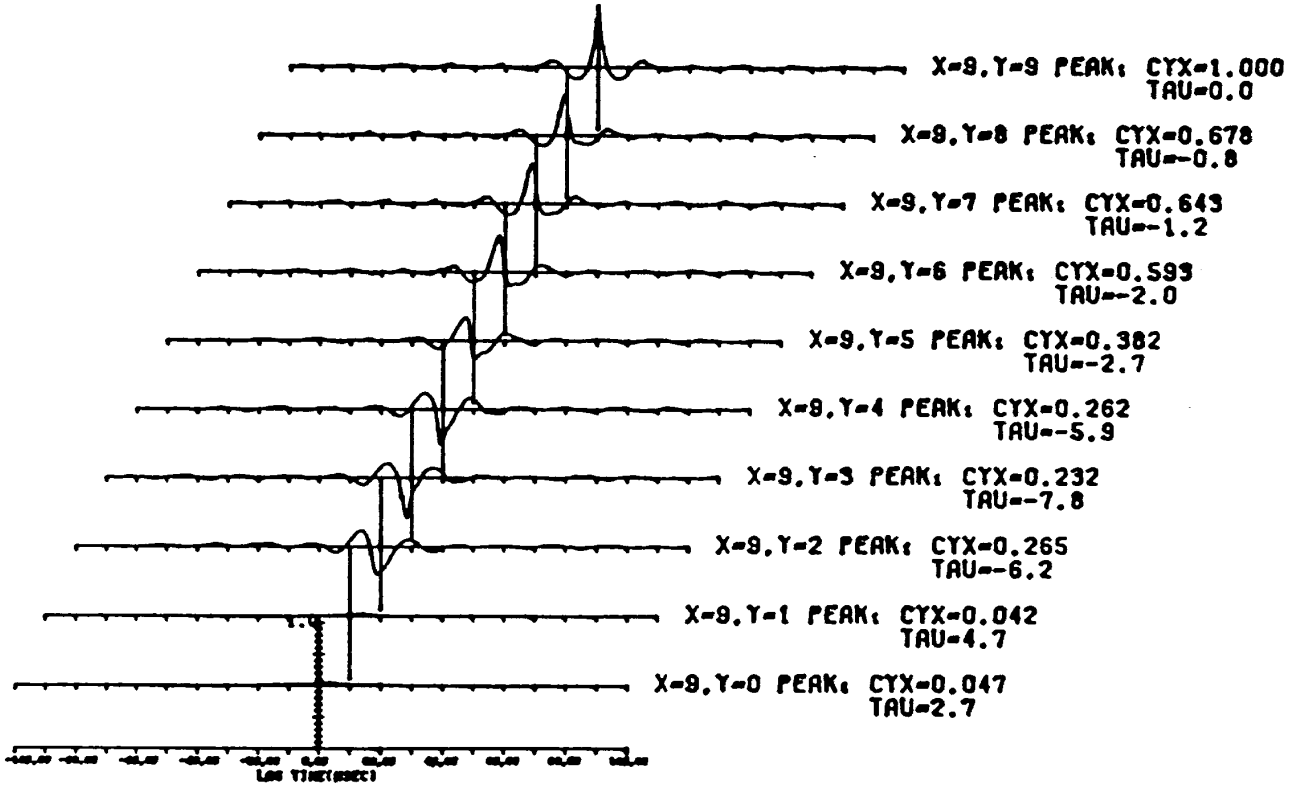

Fig. 7 Power spectra and cross-correlations
NACA0012 airfoil, M = 0.70, $\alpha = 6^{\circ}$, Re = 15×10^6

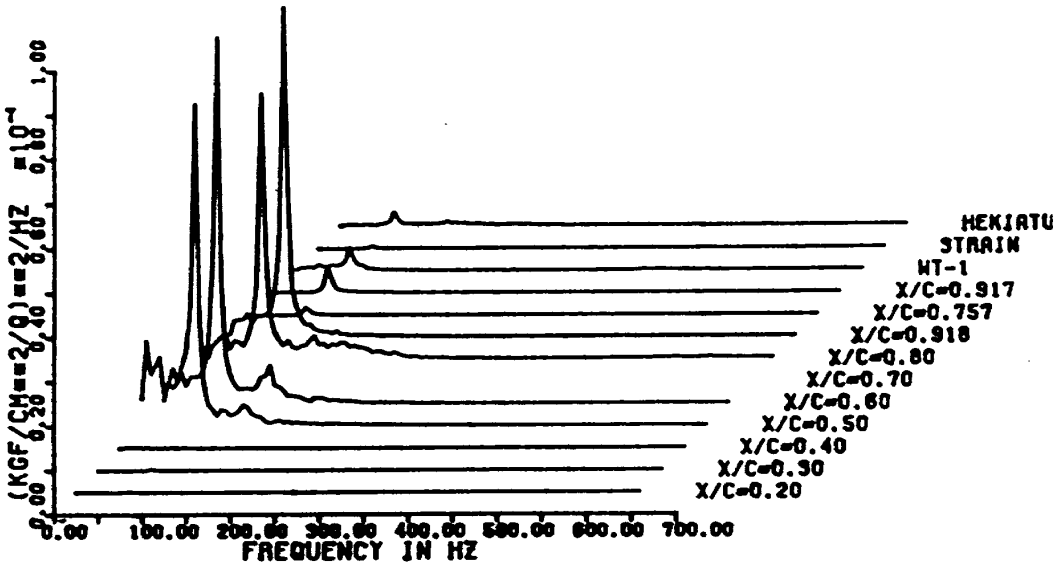

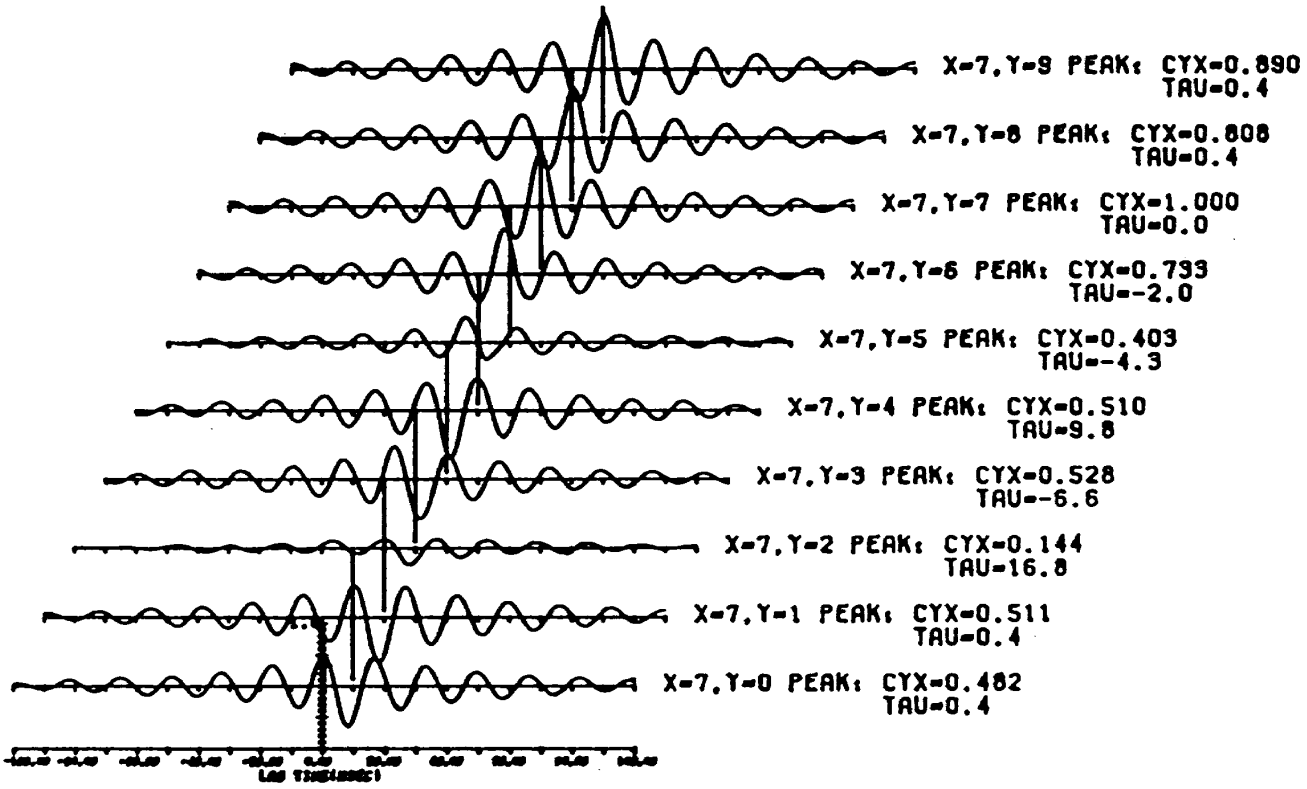

Fig. 8 Power spectra and cross-correlations
KORN airfoil, M = 0.75, $\alpha = 4^\circ$, Re = 30×10^6

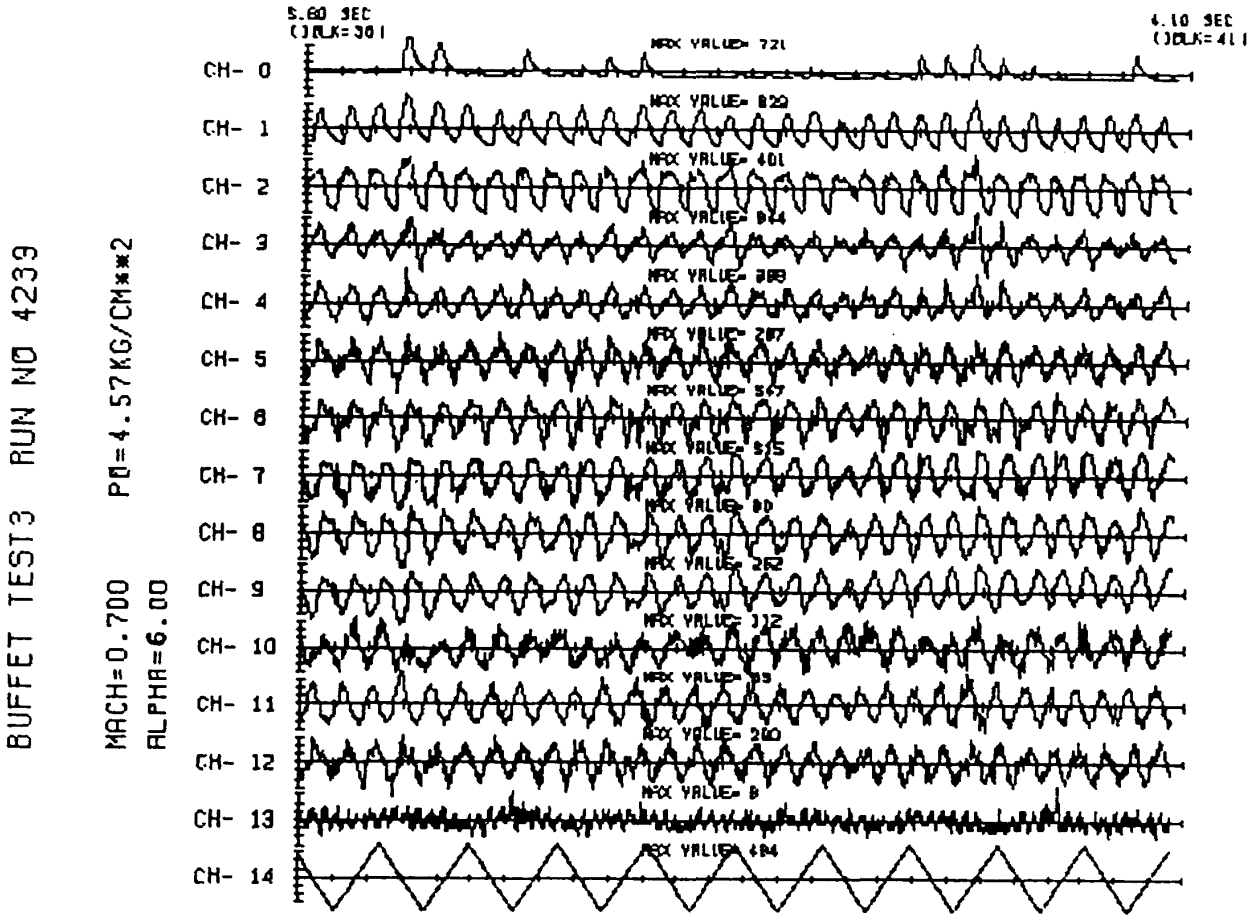

Fig. 9 Time history of pressure fluctuation
KORN airfoil, M = 0.70, $\alpha = 6^\circ$

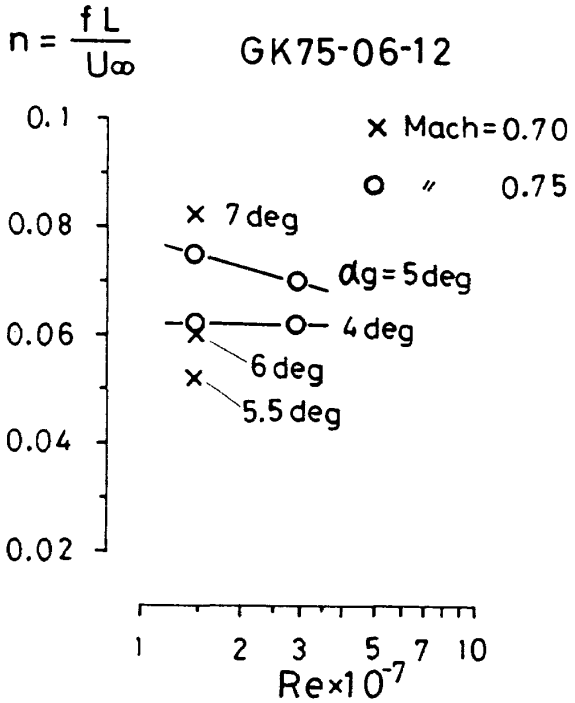

Fig. 10 Strouhal number of separated vortices
KORN airfoil

Reynolds number increases, sharp peak of mono-frequency (60 Hz) is observed and periodic cross-correlation is obtained as shown in the figure. Time history of pressure fluctuation in Fig. 9 shows that periodic organized separated vortices are formed behind the shock wave when Reynolds number is high. Figure 10 shows this votex shedding Strouhal number n based upon chord length and free stream velocity is about 0.06 ~ 0.08 depending on angle of attack and is nearly independent of Reynolds number.

3. COMPUTATIONAL RESEARCH

3.1 Navier-Stokes Code

Two-dimensional code based on Implicit Approximate Factorization scheme for time-averaged thin-layer Navier-Stokes equations was used in the computational research.[7] The turbulence

model applied is conventional Baldwin-Lomax algebraic model.[9] The details of numeric scheme and turbulence model can be found in the references. For computation of flow with laminar to turbulent transition (terms as 'transitional flow'), Baldwin's criterion of transition; max. $\mu_t < C_{MUTM} = 14$, was employed. A 'fully turbulent' computation was made assuming flow was turbulent from leading edge both sides. A relaxation model of eddy viscosity is also employed in the wake region.

3.2 Computing and Flow Conditions

Computations were made for NACA0012 airfoil to see the effects of Reynolds number, angle of attack, transition models on buffet. A C-type mesh of 133 × 49 points covering the computing region size of 10 chord length from airfoil in each direction was used. 93 points lie over the airfoil. The minimum normal size of mesh is 1×10^{-5}, streamwise size at the leading edge is 0.007 where length scale is normalized to chord length. In the following discussion, time scale is normalized using chord length and free stream velocity.

Flow conditions were M = 0.75, $\alpha = 0 \sim 6°$, Re = 1, 10, 50 × 10^6. Fully turbulent flow and transitional flow were compared.

KORN airfoil computations were made using similar mesh with leading edge streamwise width 0.0025 to cover the subtle geometry of the supercritical airfoil. Flows at Re = 6 × 10^6 and transitional model were computed for M = 0.60 ~ 0.95 and angles of attack to cover buffet region.

3.3 Results and Discussion

3.3.1 NACA0012 analysis

[LIFT CHARACTERISTICS]

Transition point at low Reynolds number is located in front of shock wave at midchord and this strongly affects pressure and friction force distributions and lift characteristics compared

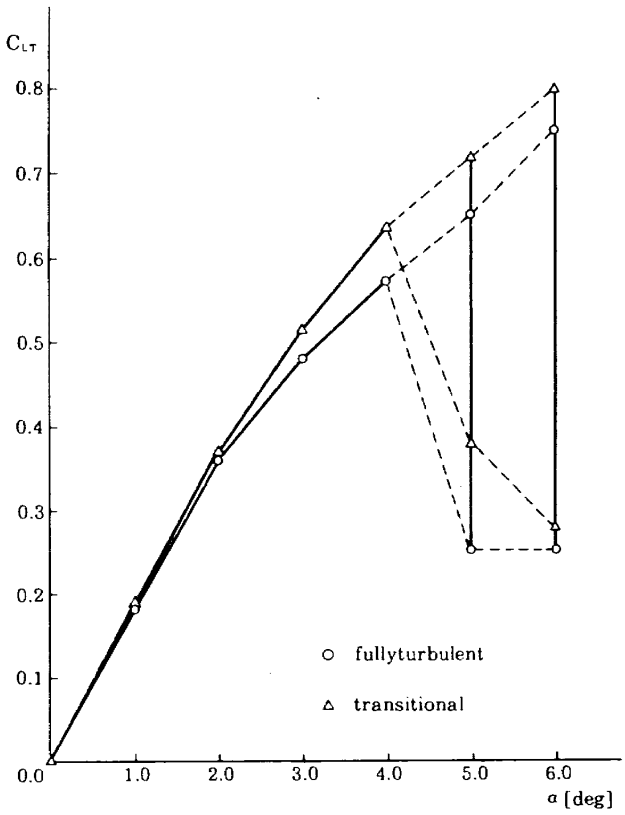

Fig. 11 C_l vs. α.
NACA0012 airfoil, Re = 1 × 10^6
○ fully turbulent
△ transitional

with fully turbulent case. Figure 11 shows C_l vs. α at Re = 1 × 10^6. Transitional flow (△) gives higher lift at nonlinear range, $\alpha \geqq 2°$, than fully turbulent flow (○). Buffet onset point is the same at $\alpha = 5°$, but the range of C_l oscillation differs. Figure 12 compares Mach number contours at fully turbulent (a) and transitional (b) cases at $\alpha = 4°$. The difference in boundary layer development and shock position can easily be seen. At Re = 10 × 10^6, the transition point locates before 0.04 C. Therefore, the boundary layer development differs little from fully turbulent case. C_l vs. α curve almost coincides with each other. Buffet onset point is 6°.

[UNSTEADY FORCE CHARACTERISTICS]

Unsteady aerodynamic forces were plotted against time in Fig. 13. Symbols ○, □ and △ represent C_l, C_d and C_m, respectively. (a) is the case: $\alpha = 5°$, fully turbulent, Re = 1 × 10^6.

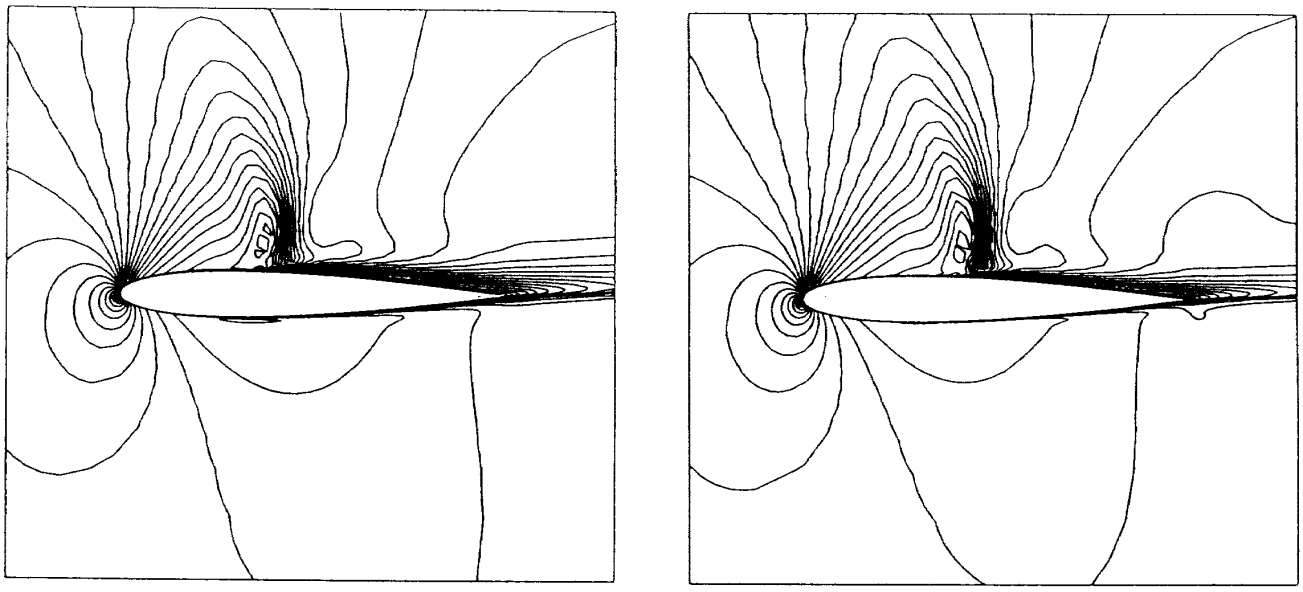

(a) fully turbulent (b) transitional

Fig. 12 Mach number contours, NACA0012, $\alpha = 4^\circ$, $Re = 1 \times 10^6$

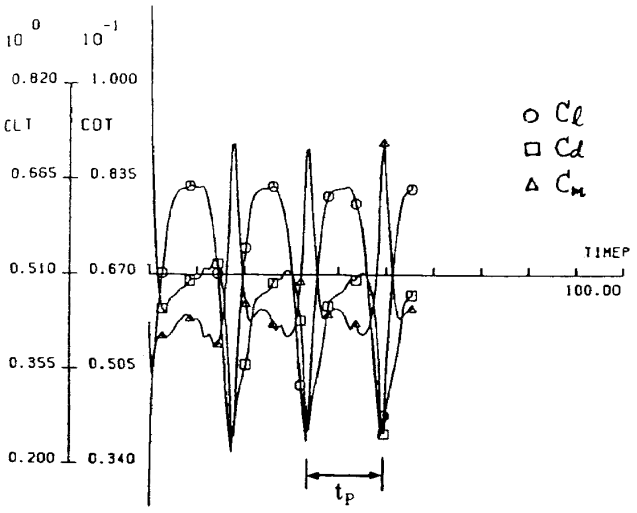

(a) $\alpha = 5^\circ$, fully turbulent, $Re = 1 \times 10^6$

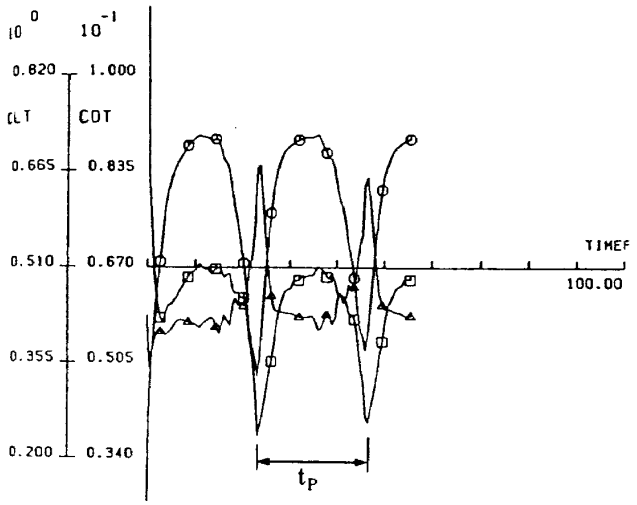

(b) transitional, $Re = 1 \times 10^6$

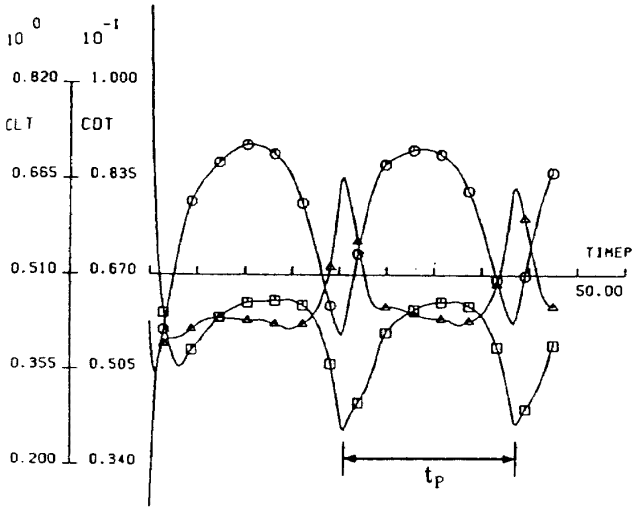

(c) fully turbulent, $Re = 50 \times 10^6$

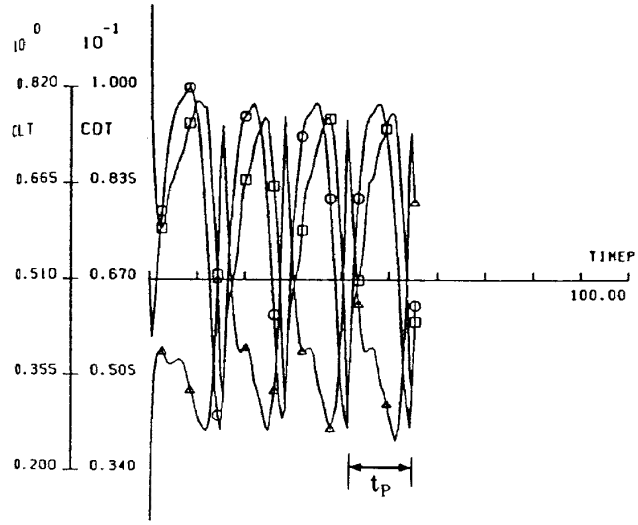

(d) $\alpha = 6^\circ$, transitional, $Re = 1 \times 10^6$

Fig. 13 Unsteady force characteristics vs. time
○: C_l, □: C_d, △: C_m

Only one parameter was changed in the other cases. (b): transitional, (c): Re = 50 × 10^6, (d): α = 6°, transitional. As opposed to the speculation from the previous result,[8] it was found that the periodic oscillation curves are not simple sinusoidal. At low Reynolds number where transition effect is significant, curve is complicated.

Although more detailed study is required, the obtained result roughly shows that:

as Re increases ⇒ T_p increases (T_p: basic period)
fully turb. → trans. ⇒ T_p increases
as α increases ⇒ T_p decreases
as Re increases ⇒ $\alpha_{buffet\ onset}$ increases and
$\Delta C_l, \Delta C_d$ decreases
fully turb. → trans. ⇒ ΔC_l, ΔC_d decreases
Typical T_p = 22 (α = 5°, fully turb.) to, 31 (α = 5°, trans.)
4–5 times longer than supercritical airfoil case (T_p = 5.54)[8]

[PRESSURE FLUCTUATION CAUSED BY TRANSITION]

When transition point locates mid-chord in low Reynolds number flow, pressure fluctuation starts to appear at α = 4° before buffet onset and can be observed as small C_l oscillation. At high Reynolds number flow, it disappears. To confirm this is physical, and not numerical oscillation, transition point X_{tr}, C_{PTE}, C_d, and C_p at X_{lower} = 0.19, and X_{upper}, X_{lower} = 0.75 were plotted against time-step number in Fig. 14 (α = 4°, transitional). X_{tr} on lower surface moves

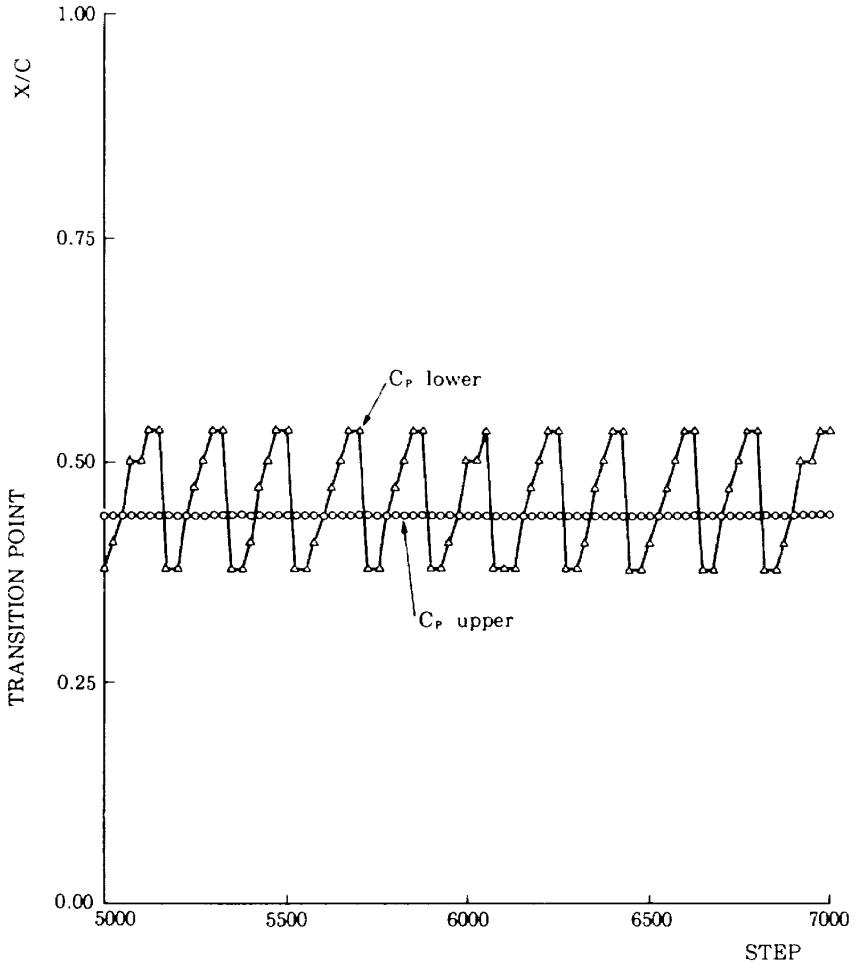

(a) transition point X_{tr}

Fig. 14 Unsteady fluctuations vs. time
NACA0012, M = 0.75, Re = 1 × 10^6, α = 4°, transitional

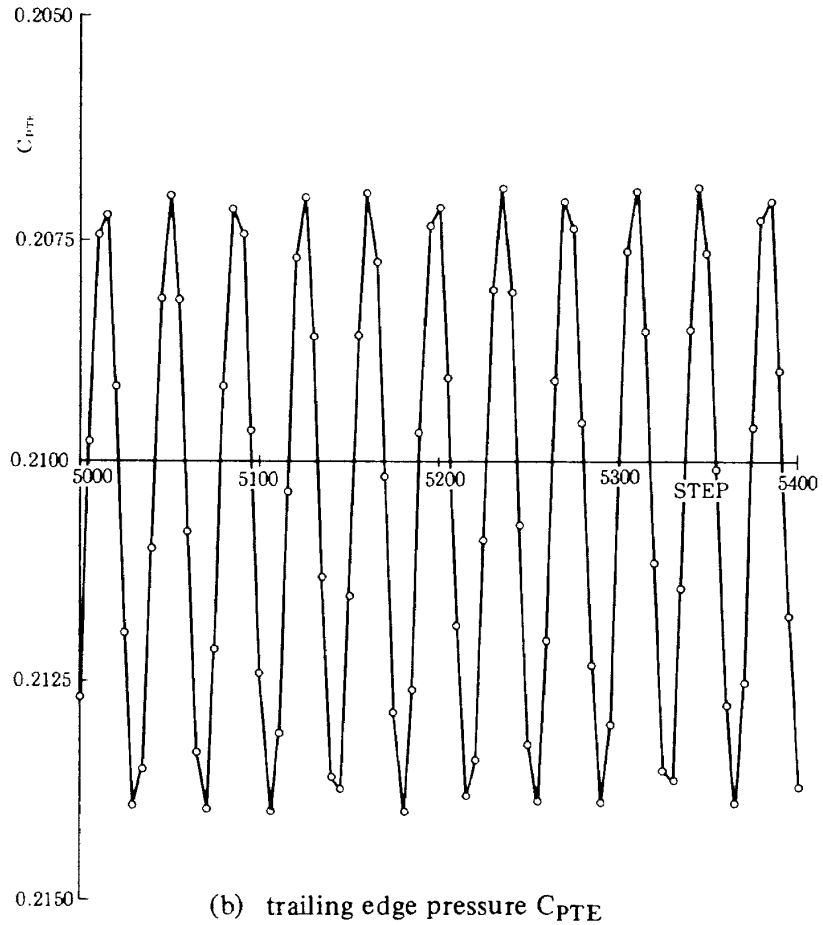

(b) trailing edge pressure C_{PTE}

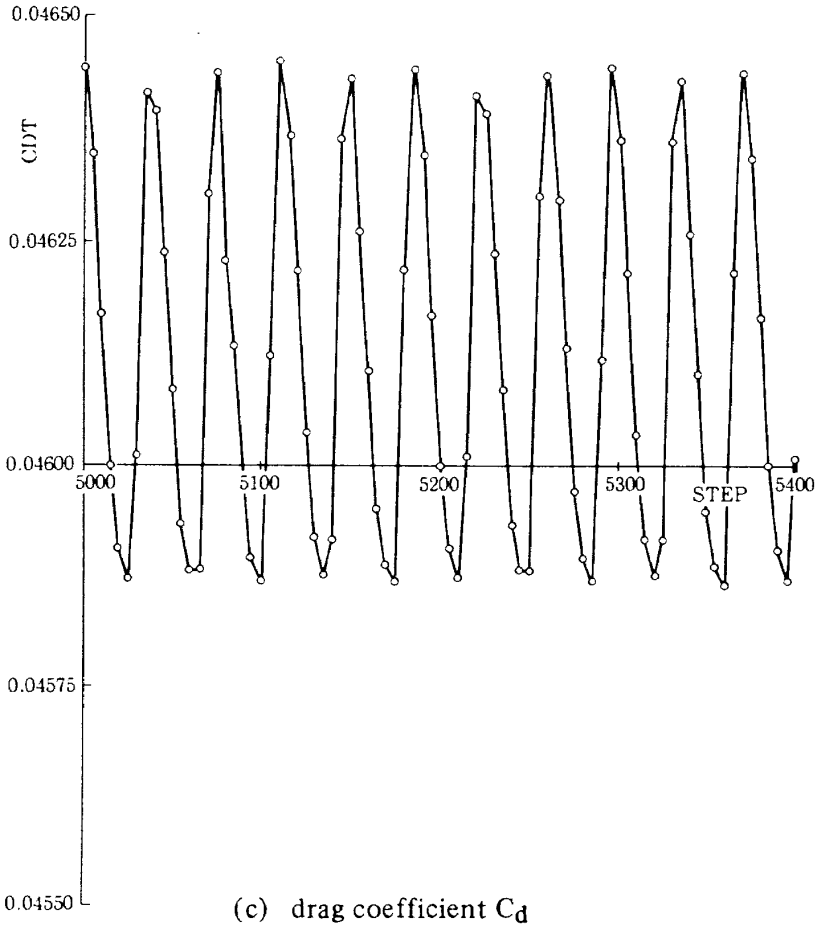

(c) drag coefficient C_d

Fig. 14 (Continued)

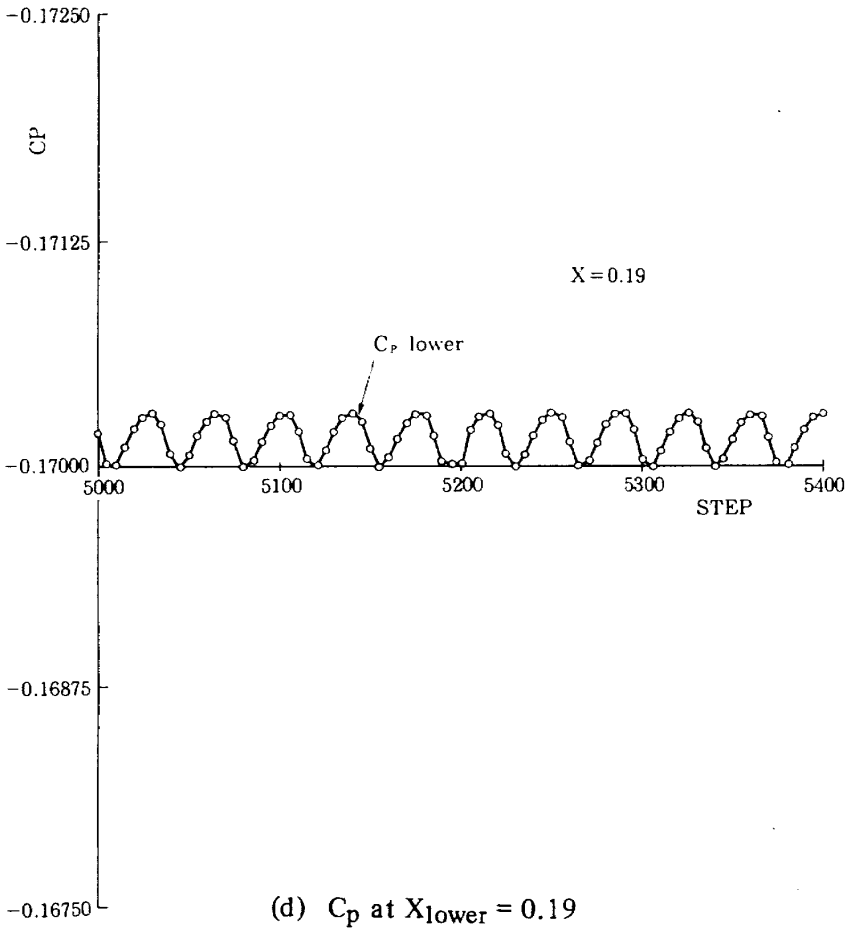

(d) C_p at $X_{lower} = 0.19$

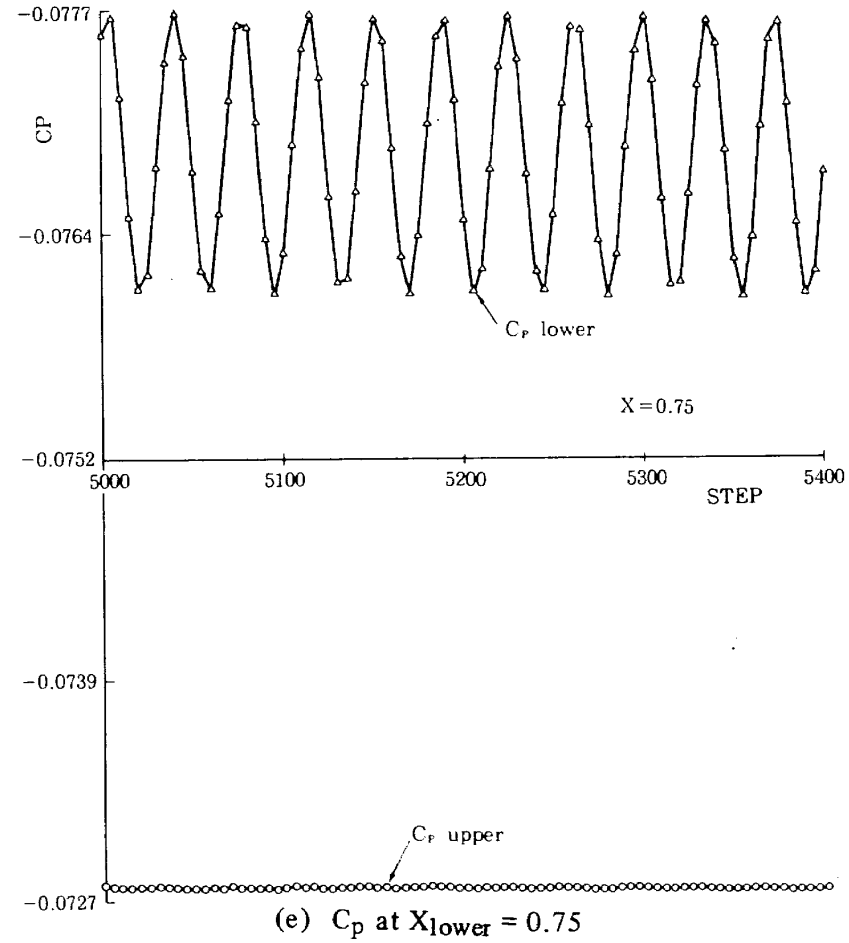

(e) C_p at $X_{lower} = 0.75$

Fig. 14 (Continued)

from 0.40 to 0.56 C with period $p_{short} = 0.47$. C_{PTE} and C_d synchronously oscillate with the same period. C_p at $X_{lower} = 0.19$ where is laminar and C_p at $X_{lpwer} = 0.75$ where is turbulent are also synchronized and amplitudes show large difference. C_p also has long period mode oscillation of $p_{long} = 2.89$. Such unsteadiness appears on the subcritical lower surface at $\alpha \geqq 1°$ and cannot be found in the supercritical upper surface and high Reynolds number flow in which transition occurs near the leading edge.

When buffet starts, such small fluctuation is overwhelmed by large scale votex shedding. Trailing edge pressure, however, seems to retain some influences. Figure 15 shows C_{PTE} for fully turbulent and transitional cases. High frequency

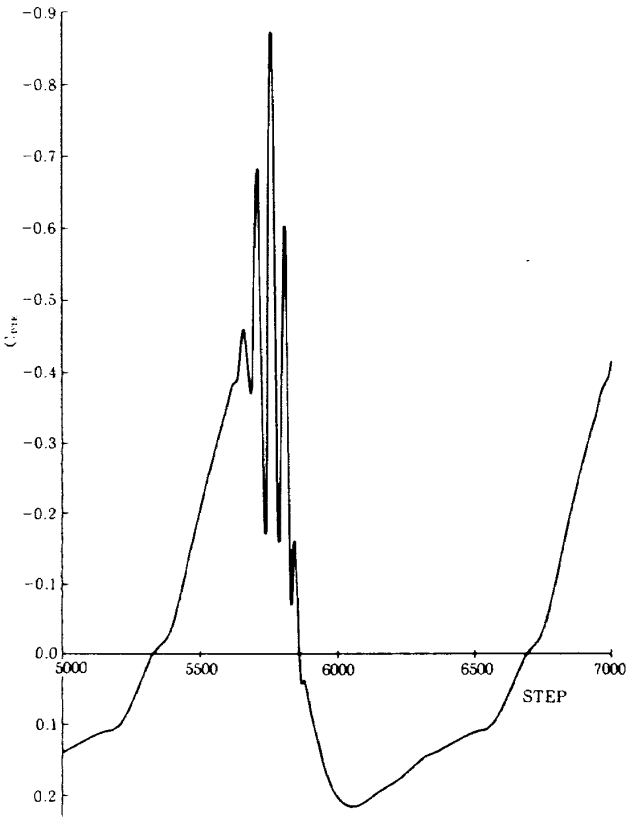

(a) fully turbulent

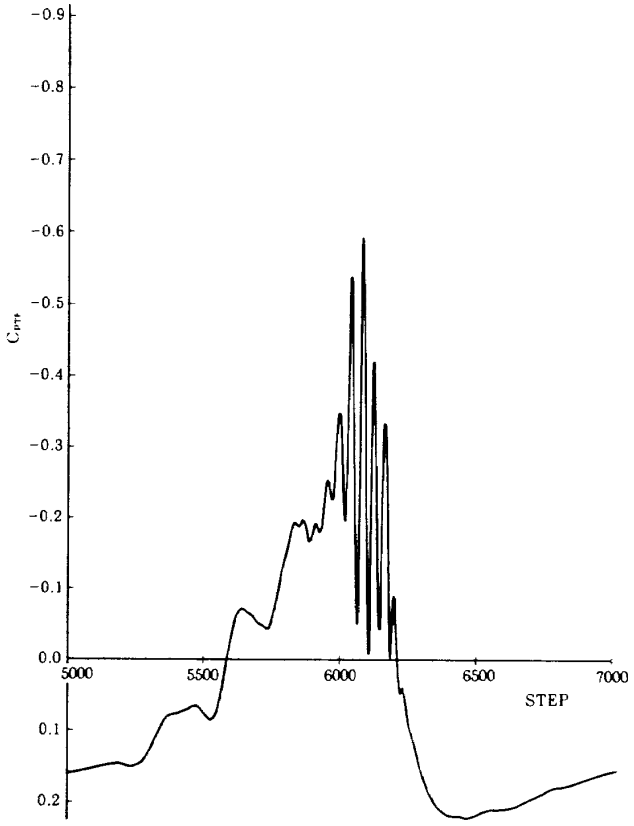

(b) transitional

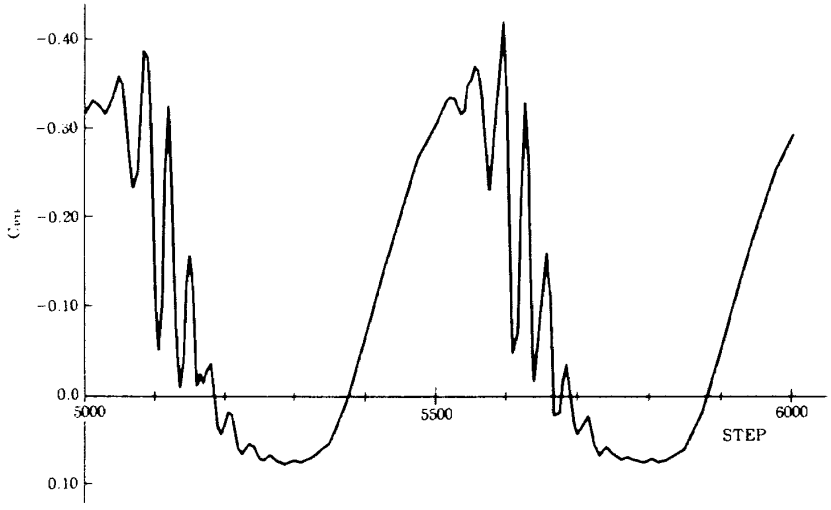

(c) a supercritical airfoil[8]

Fig. 15 Trailing edge pressure C_{PTE} vs. time
NACA0012, M = 0.75, Re = 1 × 10^6, $\alpha = 5°$

modes appears in latter case. Another supercritical airfoil case is also shown for comparison.

[VORTEX SHEDDING PATTERN]

Time dependent vortex shedding was examined plotting velocity vectors and variable contours at discretized phase angles. The scale of vortex and pressure fluctuation were greater in fully turbulent flow than in transitional flow.

The vortex at the foot of the shock wave grows larger as the chock wave moves forward until the separated region is large enough to stop the shock wave movement. Just after the shock wave stops and begins to move backward, vortex leaves airfoil and floats down in the stream. C_{PTE} becomes minimum and oscillates at this moment. After vortex is shedded, flow behind the shock wave becomes attached and shock wave is pulled down to backward. C_{PTE} regains positive pressure.

3.3.2 KORN airfoil analysis

[LIFT CHARACTERISTICS]

Figure 16(a) shows lift characteristics vs. α with Mach number as a parameter. At buffet region, maximum and minimum C_l are plotted to represent the amplitude of buffet. This amplitude nearly corresponds to the shock wave location width because lift is mostly created by supercritical region in front of shock wave. The amplitude is larger at low Mach number and almost deceases when $M \geqq 0.85$. Buffet disappears at M = 0.90. Buffet range in terms of angle of attack is plotted against Mach number in Fig. 16(b). This result is in excellent agreement with the experimental result.

[BUFFET PATTERNS]

Unsteady forces against time were plotted in Fig. 17 with typical Mach number contours at several Mach numbers. Buffet pattern and shock wave shape are quite different as Mach number increases. At low Mach numbers, buffet is similar to the low speed stall phenomena. Large scale vortices appear over the entire upper surface. Turbulence model for separated region greatly influences the solution and the present results only give qualitative pattern of separation with too large eddy viscosity. At M = 0.75, shock wave locates in relatively flat midchord surface. Shock-induced separation is not extended so large. Oscillation is simply sinusoidal as was the previous supercritical airfoil. For higher Mach number, fish-tail shock wave locates near the trailing edge and buffet deceases.

When compared in detail, shock wave location width is greater in computation than in

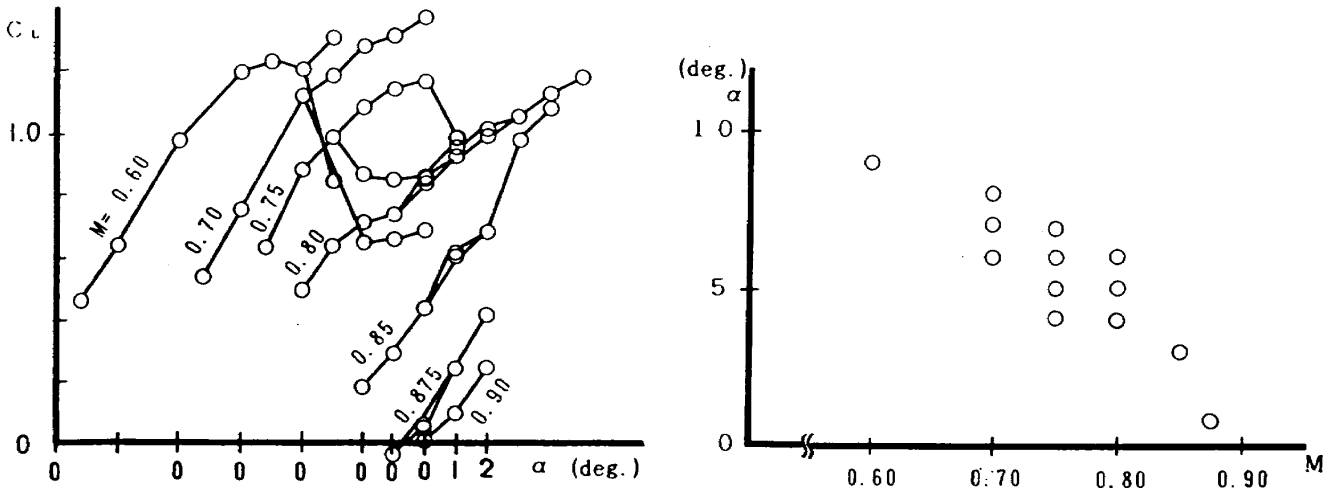

(a) lift characteristics vs. α (b) buffet range

Fig. 16 Buffet characteristics of KORN airfoil
Re = 6×10^6, transitional

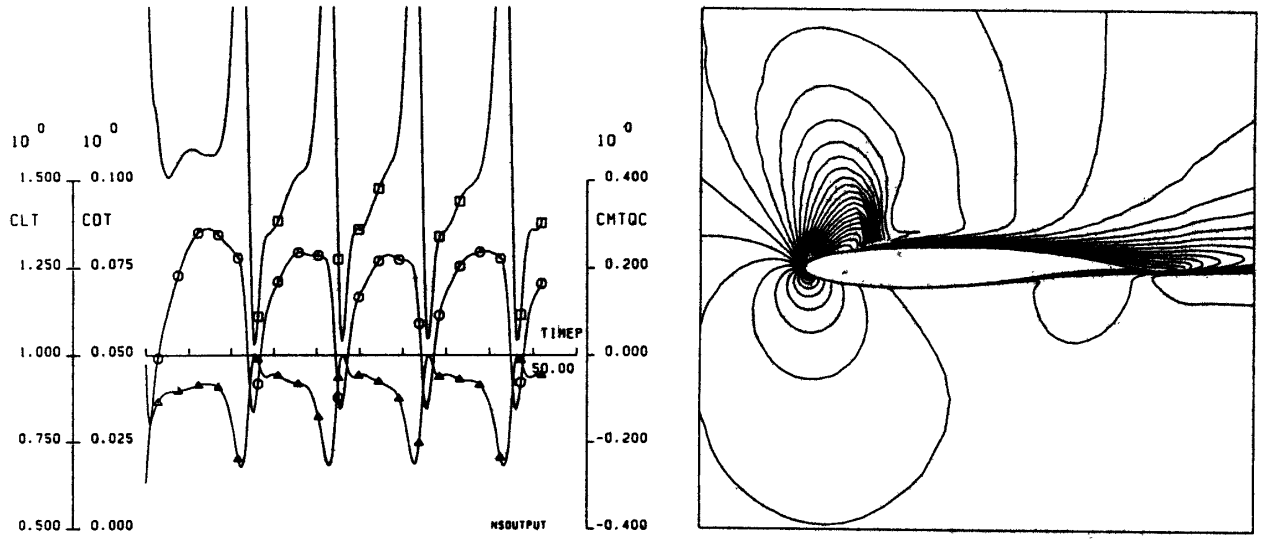

(a) M = 0.60, $\alpha = 9^\circ$

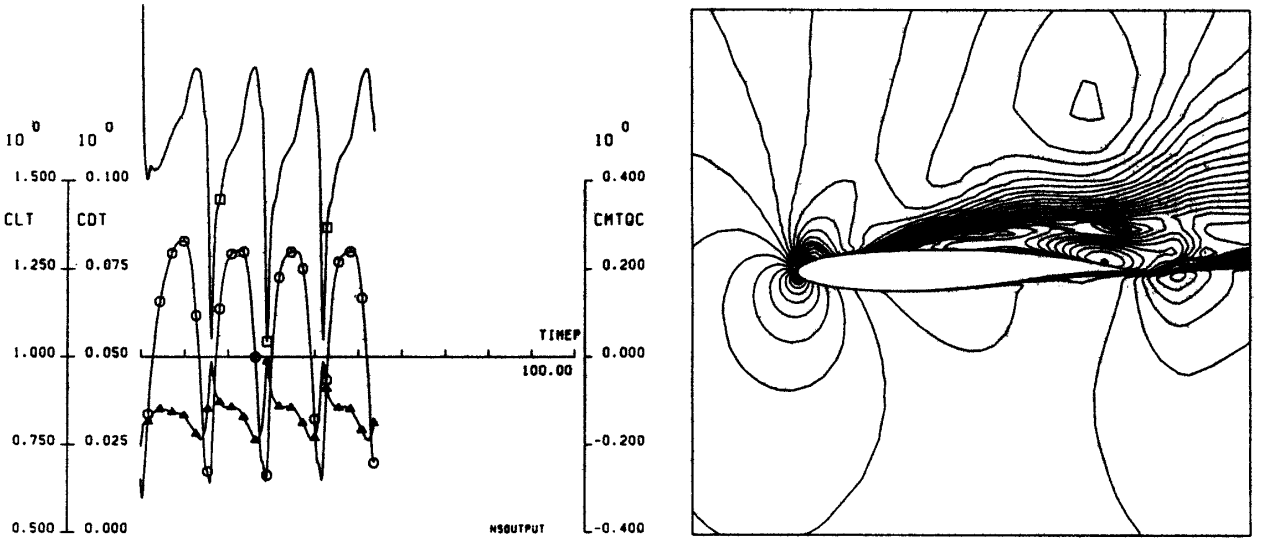

(b) M = 0.70, $\alpha = 7^\circ$

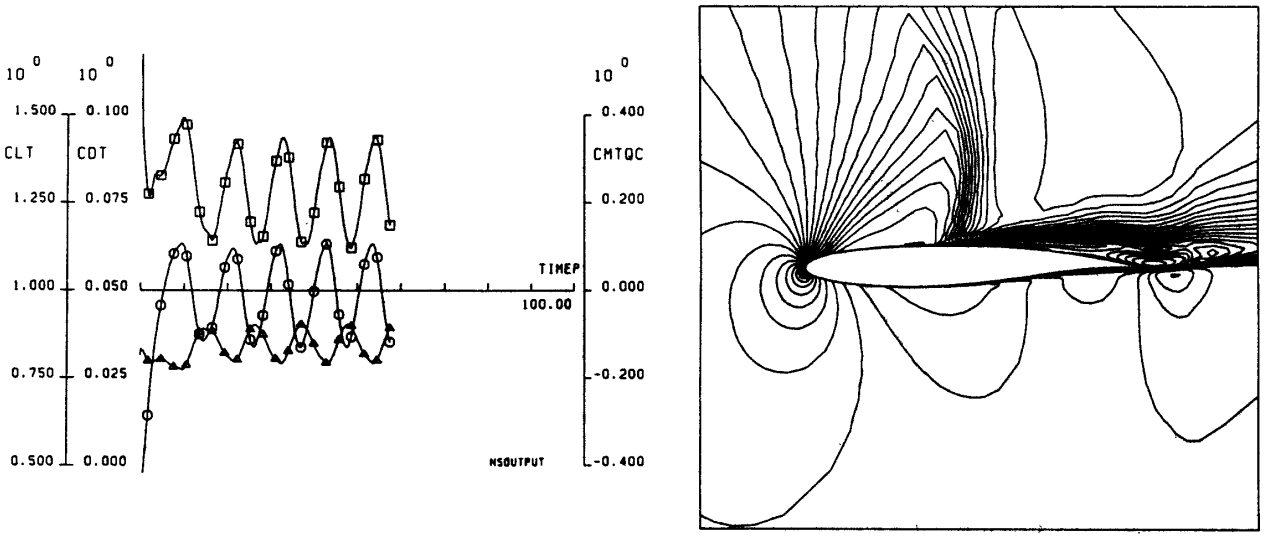

(c) M = 0.75, $\alpha = 5^\circ$

Fig. 17 Unsteady force characteristics vs. time and Mach number contours, KORN airfoil

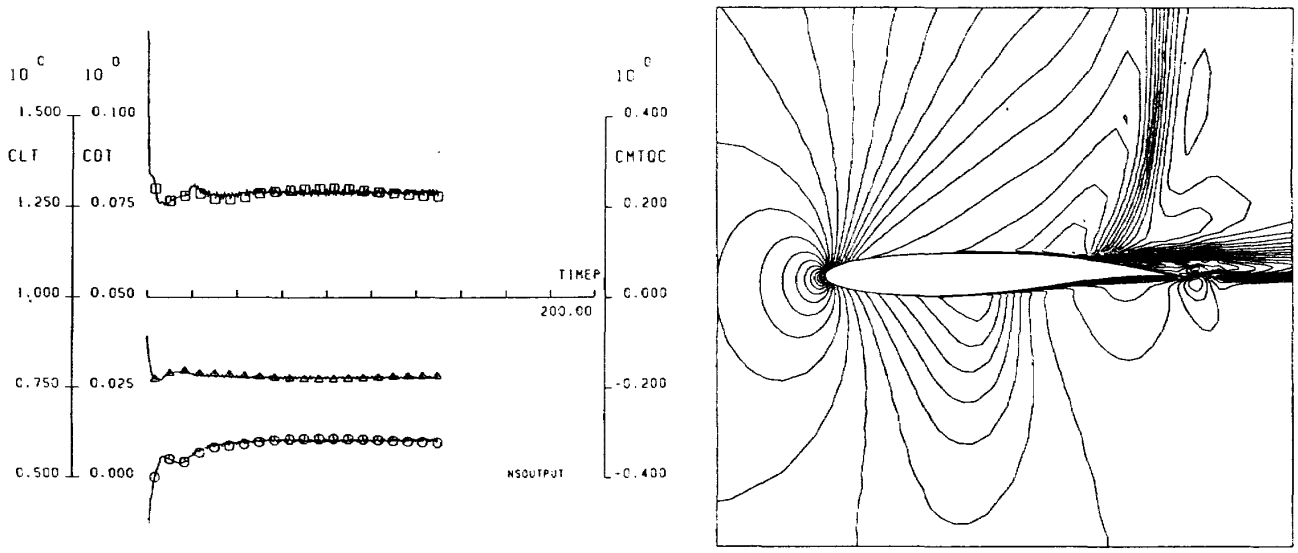

(d) M = 0.85, $\alpha = 3°$

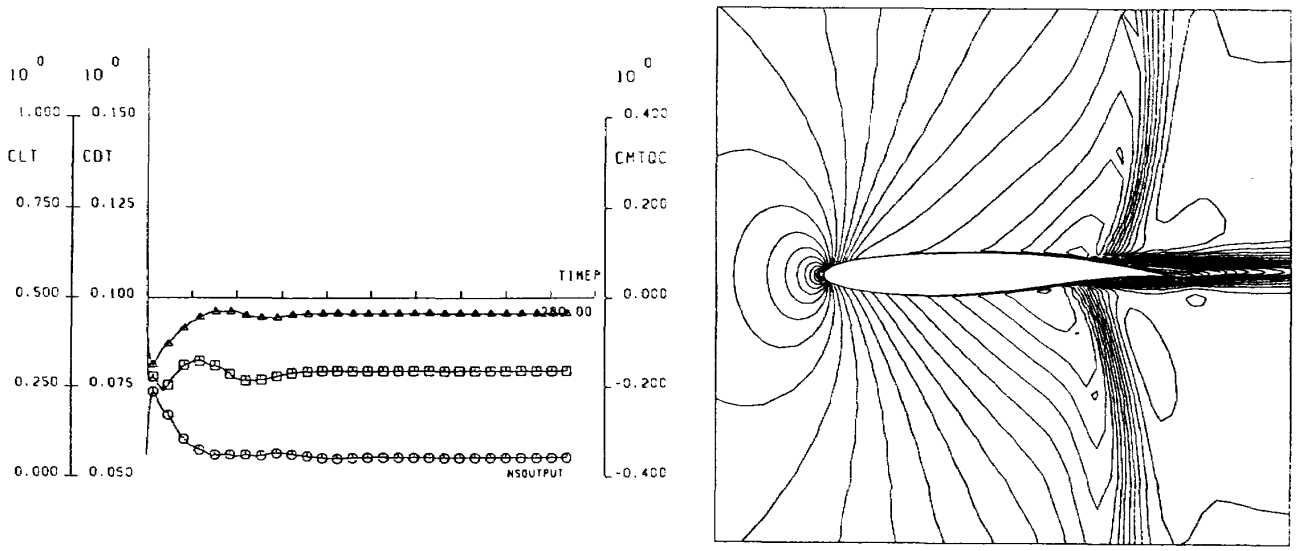

(e) M = 0.875, $\alpha = 0.831°$

Fig. 17 (Continued)

experiment. Present computation has poor resolution for shock wave. Turbulence model has large effect. In experiment, finding extreme edges of shock wave movement is difficult. Transition point is not clear. Those and other factors should be examined in future.

4. CONCLUDING REMARKS

Differences in various aspects were observed between NACA0012 and KORN airfoils in experimental research. Airfoil geometry and the resultant pressure distribution are the reasons of differences and supercritical airfoil gives more favorable buffet characteristics than conventional one. Computations revealed another aspects of buffet phenomena. Marco scale characteristics such as buffet boundary and shock wave location agreed well with experiment. Unsteady flow characteristics, however, exhibit both of agreement and disagreement. For example, Reynolds number effect on periodicity in NACA0012 is opposite. Two factors influencing the computed result are: evaluation of transition point and turbulence model for

separated region. A refined model and fine mesh analysis should be done in future. Advanced experiment is scheduled to attain good two-dimensionality and direct pressure measurement at surface.

ACKNOWLEDGMENT

The authors express their thanks to Division Chief Mr. K. TAKASHIMA, Dr. I. KAWAMOTO, Messrs. Y. OGUNI, M. SATO, H. KANDA, and N. KAWAI, and J. MIYAKAWA (MHI) and Prof. R. KAWAMURA and Mr. Y. MATSUMOTO (Nihon Univ.) for their contributions in experiments, computations and helpful discussions.

The present paper was prepared for the presentation at the IUTAM Symposium TRANSSONICUM III, Göttingen, May 24-27, 1988.

The authors also express their gratitude to Prof. Isao IMAI, Member of IUTAM International Committee, and NAL Director Mr. H. NAGASU and Division Chief Mr. K. TAKASHIMA for their support of the presentation at the Symposium.

REFERENCES

1) McDEVITT, J.B., LEVY Jr., L.L. & DEIWERT, G.S., "Transonic Flow about a Thick Circular-Arc Airfoil", AIAA J. **14**, No. 5, 606-613, (1976).
2) LEVY Jr., L.L., "Experimental and Computational Steady and Unsteady Transonic Flows about a Thick Airfoil", AIAA J. **16**, No. 6, 564-572, (1978).
3) SEEGMILLER, H.L., MARVIN, J.G. & LEVY Jr., L.L., "Steady and Unsteady Transonic Flow", AIAA J. **16**, No. 12, 1262-1269, (1978).
4) LEVY Jr., L.L. & BAILEY, H.E., "Computation of Airfoil Buffet Boundaries", AIAA J. **19**, No. 11, 1488-1490, (1981).
5) ROOS, F.W., "Some Features of the Unsteady Pressure Field in Transonic Airfoil Buffeting", J. Aircraft **17**, No. 11, 781-788, (1980).
6) TAKASHIMA, K., "Experimental Works in the NAL High Reynolds Number Two-Dimensional Transonic Wind Tunnel on Advanced Technology and NACA Airfoils", ICAS-Paper No. 82-5-4-4, (1982).
7) KAWAI, N. & HIROSE, N., "Development of the Code NSFOIL for Analyzing High Reynolds Number Transonic Flow Around An Airfoil", NAL-TR-816, (1984).
8) MIYAKAWA, J., HIROSE, N. & KWAI, N., "Comparison of Transonic Airfoil Characteristics by Navier-Stokes Computation and by Wind Tunnel Test at High Reynolds Number", AIAA Paper 85-5025, (1985).
9) BALDWIN, B.S. & LOMAX, H., "Thin Layer Approximation and Algebraic Model for Separated Turbulent Flows", AIAA Paper 78-257, (1978).

TECHNICAL REPORT OF NATIONAL
AEROSPACE LABORATORY
TR-996T

航空宇宙技術研究所報告996T号（欧文）

昭和63年9月発行

発行所　航空宇宙技術研究所
東京都調布市深大寺東町7丁目44番地1
電話三鷹(0422)47-5911（大代表）〒182
印刷所　株式会社　東京プレス
東京都板橋区桜川2－27－12

Published by
NATIONAL AEROSPACE LABORATORY
1,880 Jindaiji, Chōfu, Tokyo
JAPAN

Printed in Japan